

Dear Author,

Here are the proofs of your article.

- You can submit your corrections **online**, via **e-mail** or by **fax**.
- For **online** submission please insert your corrections in the online correction form. Always indicate the line number to which the correction refers.
- You can also insert your corrections in the proof PDF and **email** the annotated PDF.
- For fax submission, please ensure that your corrections are clearly legible. Use a fine black pen and write the correction in the margin, not too close to the edge of the page.
- Remember to note the **journal title**, **article number**, and **your name** when sending your response via e-mail or fax.
- **Check** the metadata sheet to make sure that the header information, especially author names and the corresponding affiliations are correctly shown.
- **Check** the questions that may have arisen during copy editing and insert your answers/ corrections.
- **Check** that the text is complete and that all figures, tables and their legends are included. Also check the accuracy of special characters, equations, and electronic supplementary material if applicable. If necessary refer to the *Edited manuscript*.
- The publication of inaccurate data such as dosages and units can have serious consequences. Please take particular care that all such details are correct.
- Please **do not** make changes that involve only matters of style. We have generally introduced forms that follow the journal's style. Substantial changes in content, e.g., new results, corrected values, title and authorship are not allowed without the approval of the responsible editor. In such a case, please contact the Editorial Office and return his/her consent together with the proof.
- If we do not receive your corrections **within 48 hours**, we will send you a reminder.
- Your article will be published **Online First** approximately one week after receipt of your corrected proofs. This is the **official first publication** citable with the DOI. **Further changes are, therefore, not possible.**
- The **printed version** will follow in a forthcoming issue.

Please note

After online publication, subscribers (personal/institutional) to this journal will have access to the complete article via the DOI using the URL: [http://dx.doi.org/\[DOI\]](http://dx.doi.org/[DOI]).

If you would like to know when your article has been published online, take advantage of our free alert service. For registration and further information go to: <http://www.springerlink.com>.

Due to the electronic nature of the procedure, the manuscript and the original figures will only be returned to you on special request. When you return your corrections, please inform us if you would like to have these documents returned.

Metadata of the article that will be visualized in OnlineFirst

Please note: Images will appear in color online but will be printed in black and white.

ArticleTitle	Spatial oxygen heterogeneity in a <i>Hediste diversicolor</i> irrigated burrow	
Article Sub-Title		
Article CopyRight	Springer Science+Business Media B.V. (This will be the copyright line in the final PDF)	
Journal Name	Hydrobiologia	
Corresponding Author	Family Name	Gilbert
	Particle	
	Given Name	Franck
	Suffix	
	Division	EcoLab, Laboratoire d'Ecologie Fonctionnelle et Environnement, UPS, INP
	Organization	Université de Toulouse
	Address	118 route de Narbonne, 31062, Toulouse Cedex 9, France
	Division	
	Organization	EcoLab,CNRS
	Address	31055, Toulouse, France
	Email	franck.gilbert@cict.fr
Author	Family Name	Pischedda
	Particle	
	Given Name	Laura
	Suffix	
	Division	Laboratoire de Microbiologie, Géochimie et Ecologie Marines (UMR CNRS 6117), Centre d'Océanologie de Marseille
	Organization	Université de la Méditerranée
	Address	Campus de Luminy, Case 901, 13288, Marseille Cedex 9, France
	Email	
Author	Family Name	Cuny
	Particle	
	Given Name	Philippe
	Suffix	
	Division	Laboratoire de Microbiologie, Géochimie et Ecologie Marines (UMR CNRS 6117), Centre d'Océanologie de Marseille
	Organization	Université de la Méditerranée
	Address	Campus de Luminy, Case 901, 13288, Marseille Cedex 9, France
	Email	
Author	Family Name	Esteves
	Particle	
	Given Name	José Luis
	Suffix	
	Division	Centro Nacional Patagónico, Unidad de Investigación de Oceanografía y Meteorología, Laboratorio de Oceanografía Química y Contaminación de Aguas
	Organization	CONICET

	Address	Bv. Brown 2825, U9120ACF, Puerto Madryn, Argentina
	Email	
Author	Family Name	Poggiale
	Particle	
	Given Name	Jean-Christophe
	Suffix	
	Division	Laboratoire de Microbiologie, Géochimie et Ecologie Marines (UMR CNRS 6117), Centre d'Océanologie de Marseille
	Organization	Université de la Méditerranée
	Address	Campus de Luminy, Case 901, 13288, Marseille Cedex 9, France
	Email	
Schedule	Received	18 May 2011
	Revised	12 September 2011
	Accepted	25 September 2011
Abstract	<p>The heterogeneity of oxygen distribution in a <i>Hediste diversicolor</i> burrow environment was investigated in a laboratory experiment using a 6-mm thick tank equipped with oxygen planar optodes. The two-dimensional oxygen distribution in a complete burrow was monitored every 2 min for 4 h. Oxygen concentrations fluctuated over a scale of minutes in the burrow lumen and wall (up to 2 mm) reflecting the balance between worm ventilation activity and oxygen consumption. The magnitude of the three surrounding micro-horizons (oxic, oscillating and anoxic) induced by the intermittent worm ventilation was spatially and temporally variable within the structure. Oxygen variations appeared to be controlled by distance from the sediment–water interface and the direction of water circulation. Moreover, there was an apparent ‘buffer effect’, induced by the proximity to the overlying water, which reduced the variations of lumen and wall oxygen in the upper part of the structure. These results highlight the heterogeneous distribution and dynamics of oxygen associated with <i>H. diversicolor</i> burrows and ventilation activity. They also highlight the necessity of integrating this complexity into the current burrow-base models in order to estimate the ecological importance of burrowing species in coastal ecosystems.</p>	
Keywords (separated by '-')	Bioturbation - Bio-irrigation - Oxygen heterogeneity - <i>Hediste diversicolor</i> burrow - Marine sediments	
Footnote Information	Handling editor: Pierluigi Viaroli	

Journal: 10750
Article: 907



Author Query Form

**Please ensure you fill out your response to the queries raised below
and return this form along with your corrections**

Dear Author

During the process of typesetting your article, the following queries have arisen. Please check your typeset proof carefully against the queries listed below and mark the necessary changes either directly on the proof/online grid or in the 'Author's response' area provided below

Query	Details required	Author's response
1.	Please check the orders of affiliation details.	
2.	Ninth figure caption numbered as 2 in MS hence we changed to Fig. 9. Please check and confirm and approve the edit.	

2 **Spatial oxygen heterogeneity in a *Hediste diversicolor***
3 **irrigated burrow**

4 **Laura Pischedda · Philippe Cuny ·**
5 **José Luis Esteves · Jean-Christophe Poggiale ·**
6 **Franck Gilbert**

7 Received: 18 May 2011 / Revised: 12 September 2011 / Accepted: 25 September 2011
8 © Springer Science+Business Media B.V. 2011

9 **Abstract** The heterogeneity of oxygen distribution
10 in a *Hediste diversicolor* burrow environment was
11 investigated in a laboratory experiment using a 6-mm
12 thick tank equipped with oxygen planar optodes. The
13 two-dimensional oxygen distribution in a complete
14 burrow was monitored every 2 min for 4 h. Oxygen
15 concentrations fluctuated over a scale of minutes in the
16 burrow lumen and wall (up to 2 mm) reflecting the
17 balance between worm ventilation activity and oxygen
18 consumption. The magnitude of the three surrounding
19 micro-horizons (oxic, oscillating and anoxic) induced

by the intermittent worm ventilation was spatially and 20
temporally variable within the structure. Oxygen 21
variations appeared to be controlled by distance from 22
the sediment–water interface and the direction of 23
water circulation. Moreover, there was an apparent 24
'buffer effect', induced by the proximity to the 25
overlying water, which reduced the variations of 26
lumen and wall oxygen in the upper part of the 27
structure. These results highlight the heterogeneous 28
distribution and dynamics of oxygen associated with 29
H. diversicolor burrows and ventilation activity. They 30
also highlight the necessity of integrating this com- 31
plexity into the current burrow-base models in order to 32
estimate the ecological importance of burrowing 33
species in coastal ecosystems. 34

A1 Handling editor: Pierluigi Viaroli

A2 L. Pischedda · P. Cuny · J.-C. Poggiale
A3 Laboratoire de Microbiologie, Géochimie et Ecologie
A4 Marines (UMR CNRS 6117), Centre d'Océanologie de
A5 Marseille, Université de la Méditerranée, Campus de
A6 Luminy, Case 901, 13288 Marseille Cedex 9, France

A7 J. L. Esteves
A8 Centro Nacional Patagónico, Unidad de Investigación de
A9 Oceanografía y Meteorología, Laboratorio de
A10 Oceanografía Química y Contaminación de Aguas,
A11 CONICET, Bv. Brown 2825, U9120ACF Puerto Madryn,
Argentina

A12 F. Gilbert (✉)
A13 EcoLab, Laboratoire d'Ecologie Fonctionnelle et
A14 Environnement, UPS, INP, Université de Toulouse,
A15 118 route de Narbonne, 31062 Toulouse Cedex 9, France
A16 e-mail: franck.gilbert@cict.fr

A17 F. Gilbert
A18 EcoLab, CNRS, 31055 Toulouse, France

Keywords Bioturbation · Bio-irrigation · Oxygen 35
heterogeneity · *Hediste diversicolor* burrow · 36
Marine sediments 37

Introduction 39

Macrobenthic fauna profoundly alter the distribution 40
of sediment particles, solutes and microbial commu- 41
nities, especially in coastal marine ecosystems where 42
benthic organisms are densely distributed (e.g. François 43
et al., 2002; Meile & Van Cappellen, 2003; Pappaspyrou 44
et al., 2006; Gilbert et al., 2007). Through sediment 45
reworking and irrigation, a process referred to as 46
bioturbation (*sensu* Richter, 1952), the macrofauna 47

48 directly affect the decomposition, remineralisation and
 49 preservation of organic matter in sediments (Aller,
 50 1994; Reise, 2002). In particular, the gallery-diffuser
 51 organisms burrow into otherwise anoxic sediments and
 52 actively ventilate them for respiration or feeding
 53 purposes (e.g. Anderson & Meadows, 1978; Osovitz
 54 & Julian, 2002). The sediment–water interface is
 55 increased by their burrowing activity, and in addition
 56 worm ventilation activity greatly enhances solute
 57 exchanges between the sediments and the overlying
 58 water (Fenchel, 1996; Aller, 2001; Pischedda et al.,
 59 2008).

60 Macrofaunal burrows have been extensively studied
 61 in terms of sediment reworking (e.g. Dupont et al.,
 62 2006), morphology (e.g. Davey, 1994), irrigation rate
 63 (e.g. Kristensen, 2000), solute distribution and fluxes
 64 (e.g. Kristensen & Hansen, 1999), redox oscillations
 65 (e.g. Sun et al., 2002), mineralisation rate (e.g. Aller,
 66 1994) and associated microbial communities (e.g.
 67 Pappaspyrou et al., 2006). However, the distribution
 68 and dynamics of solutes within a macrofaunal burrow
 69 structure have proven difficult to determine. Conse-
 70 quently, methods such as determinations of global
 71 exchanges between the entrance and the exit of the
 72 burrow, or local concentration measurements using
 73 microelectrode(s) at the burrow openings or localised
 74 within or in the vicinity of the burrow structure (e.g. in
 75 the burrow wall) have been developed, often in
 76 association with simultaneous active ventilation record-
 77 ing (e.g. Kristensen, 1989; Forster & Graf, 1995). Based
 78 on these data, efforts have been made to model the solute
 79 distribution in actively ventilated burrow environments.
 80 Currently, there are two main types of bio-irrigation
 81 models: the diffusive tube-irrigation model (Aller,
 82 1980), which was further improved by authors such as
 83 Boudreau & Marinelli (1994), Furukawa (2001) and
 84 Koretsky et al. (2002), and the advective pocket-
 85 injection model (Meysman et al., 2006). One significant
 86 difference between these models is that the former is
 87 relevant to muddy sediments where bio-irrigation is
 88 intrinsically driven by diffusion across the burrow wall,
 89 whereas the latter describes sandy sediments where
 90 active ventilation by worms induces the advective
 91 transport of water in the surrounding sediments due to
 92 the higher permeability of sands (Foster-Smith, 1978).

93 Due to the lack of data about solute distribution,
 94 these bio-irrigation models do not include the macro-
 95 and micro-scale heterogeneity of solute distribution
 96 within the burrow and in its immediate vicinity. The

97 introduction of planar optodes into benthic ecology
 98 now makes it possible to determine the 2D distribution
 99 and dynamics of oxygen, ammonium, pCO₂ or pH in
 100 sediments (e.g. Glud et al., 1996; Hulth et al., 2002;
 101 Stromberg & Hulth, 2003; Zhu et al., 2006). With
 102 regard to oxygen, so far only a few studies have been
 103 undertaken using planar optodes to monitor oxygen
 104 distribution and dynamics in macrofaunal burrows.
 105 For instance, Timmermann et al. (2006), Polerecky
 106 et al. (2006) and Behrens et al. (2007) reported a
 107 highly dynamic pattern of oxygen distribution in
 108 laboratory experiments with the polychaete *Arenicola*
 109 *marina*, the sand eel *Ammodytes tobianus* and the
 110 Chironomid larvae *Chironomus plumosus*, respec-
 111 tively. In shallow water environments, Wenzhöfer &
 112 Glud, (2004) reported patchiness and variability of the
 113 benthic oxygen distribution on a diel scale, primarily
 114 induced by the distinct diel pattern in *Hediste diver-*
 115 *sicolor* activity and photosynthesis. More precisely,
 116 they showed that the volume of oxic sediments around
 117 burrow structures was influenced by these changing
 118 environmental conditions, and that oxygen uptake
 119 through the burrow walls just after sunset accounted
 120 for most of the total oxygen uptake. In those studies,
 121 however, the oxygen distribution and dynamics were
 122 only quantified in particular or localised areas of the
 123 burrows, and this did not make it possible to define the
 124 oxygen heterogeneity in a complete bio-irrigated
 125 burrow.

126 *Hediste diversicolor* (OF Müller, 1776) is a poly-
 127 chaete worm widely distributed in estuarine and
 128 lagoonal habitats from North Africa to North Europe
 129 (Mettam, 1979; Gillet, 1993) at a density of 500–5,000
 130 individuals per square metre (Vedel & Riisgard,
 131 1993). This species shows high physiological toler-
 132 ance of extreme variations in environmental factors,
 133 and can grow and reproduce in different sediment
 134 types and also in stressed environments (e.g. Bartels-
 135 Hardege & Zeeck, 1990; Miron & Kristensen, 1993;
 136 Scaps, 2002). It lives in a semi-permanent U- or
 137 Y-shaped mucus-lined burrow extending 6–12 cm
 138 into muddy or sandy–muddy sediments. The worm
 139 actively ventilates its burrow structure (Kristensen,
 140 1981; Davey, 1994) with regular alternations of active
 141 ventilation periods of ~10 min followed by rest
 142 periods of ~5 min (Kristensen, 2001).

143 The aim of the present laboratory study involving
 144 planar optodes was to determine the heterogeneous 2D
 145 oxygen distribution and dynamics in different areas of

146 an entire *H. diversicolor* burrow structure, and to
 147 compare the associated oxygen penetration depth and
 148 diffusive fluxes at the surface and across the burrow
 149 sediment–water interfaces.

150 Materials and methods

151 Experimental setup

152 The *H. diversicolor* specimens used in this study
 153 (8.9 ± 2.1 cm long; mean \pm SD; $N = 19$) and the
 154 sandy-mud sediments were collected in September in
 155 the Carreau cove (Gulf of Fos, Mediterranean Sea) by
 156 shovel sampling in the Saint-Antoine canal at a depth
 157 of 0–0.5 m ($43^{\circ}22'30.40''\text{N}/4^{\circ}50'20.80''\text{E}$). In the
 158 laboratory, the worms were placed in tanks filled with
 159 the experimental sediment and aerated overlying sea-
 160 water (38 ± 0.2 psu). They were acclimatised to the
 161 experimental conditions (water temp.: $24 \pm 1^{\circ}\text{C}$,
 162 natural photoperiod) for 2 weeks before the start of
 163 the experiment.

164 Two and a half weeks before the beginning of the
 165 experiment, the four transparent sides of a polycar-
 166 bonate tank ($20 \times 20 \times 20$ cm) were fitted with
 167 square oxygen optodes which had been previously
 168 cut (19×19 cm) to fit inside the tank. A PVC cube
 169 was then inserted into the tank in order to reduce the
 170 sediment thickness to 6 mm in front of each optode
 171 and make the worms and their galleries visible. The
 172 tank was then filled with a depth of about 11 cm of
 173 sieved sediments and 6–8 cm of aerated overlying
 174 water ($24 \pm 1^{\circ}\text{C}$, 38 ± 0.2 psu). Five days later,
 175 oxygen measurements constituting the control values
 176 were performed, then the organisms ($N = 19$) were
 177 placed in the tank (T_0). They immediately started to
 178 explore their environment and construct their burrows.
 179 In order to avoid the development of a microbial
 180 biofilm on the optode, especially within the burrows
 181 that are a highly favourable microenvironment for
 182 microbial activity, oxygen measurements were done
 183 3 days after the introduction of the worms on the side
 184 of the tank where most of a burrow was visible
 185 (Fig. 1). Measurements were performed every 2 min
 186 for 4 h, and provided a time series of 121 oxygen
 187 images associated with the 121 sediment structure
 188 images used to detect the sediment–water interface.

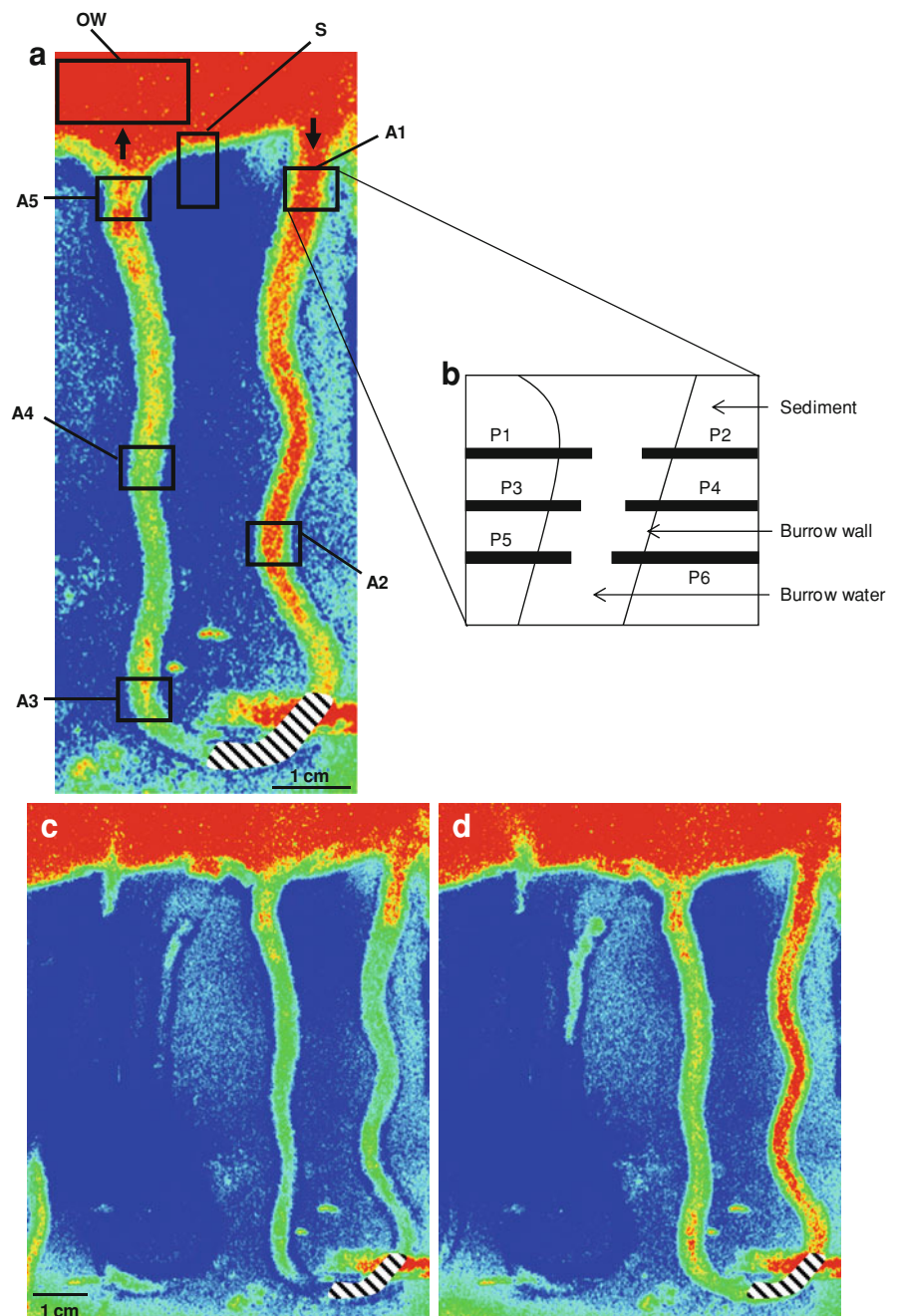
Image acquisition

190 The two-dimensional oxygen concentration in biotur-
 191 bated sediments and the overlying water was quanti-
 192 fied with semi-transparent planar oxygen optodes.
 193 Oxygen measurement was based on the dynamic
 194 quenching of oxygen on an immobilised fluorophore
 195 (Kautsky, 1939). The optical sensor was composed of
 196 two thin layers, a transparent polyester support foil
 197 (HP transparency, C2936A, ~ 150 μm thick) and a
 198 sensing layer, in which the platinum (II) mesotetra
 199 (pentafluorophenyl) porphyrin oxygen-quenchable
 200 fluorophore (Pt-PFPP, Frontier Scientific Inc.) was
 201 embedded in a polystyrene matrix (~ 20 μm)
 202 (Papkovsky et al., 1992; Liebsch et al., 2000). The
 203 sensing layer mixture was composed of 3 mg of
 204 Pt-PFPP dissolved in 3 ml of toluene (Rathburn
 205 Chemicals Ltd, Acros Organics) and 0.65 g (5%) of
 206 polystyrene pellets (Acros Organics) dissolved in
 207 15 ml of toluene. The two solutions were mixed and
 208 spread on the polyester support foil (300 cm^2). The
 209 solvent was left to evaporate slowly until the mem-
 210 brane was completely dry.

211 Oxygen optodes were calibrated by a three-point
 212 calibration method. For the two intermediate calibra-
 213 tion points (90%, air bubbling and 50%, N_2 bubbling),
 214 the oxygen concentration was first measured just
 215 behind the optode using an oxygen probe (LDO
 216 HQ10, Hach), immediately followed by capture of
 217 the oxygen image. In order to avoid problems due to
 218 uneven illumination or dye distribution (Strömberg,
 219 2006), the 0% saturation reading was taken in anoxic
 220 sediment close to the zone studied, i.e. at the sediment
 221 surface (S) or in the overlying water (OW), and in five
 222 zones of the *H. diversicolor* burrow corresponding to
 223 the inhalant opening zone (A1), two intermediate
 224 zones at mid-depth (A2 and A4), the bottom zone (A3)
 225 and the exhalant opening zone (A5), respectively
 226 (Fig. 1a). No further calibration was performed in the
 227 water environment after the experiment had begun,
 228 because it was difficult to remove sediments without
 229 damaging the optodes. However, data were corrected
 230 for drift, which was quantified on the basis of the
 231 change in the oxygen level over time in the anoxic
 232 sediment close to each of the zones studied.

233 The optical system combined with the use of the
 234 oxygen optode made it possible to take high resolution
 235 images of sediments and to measure the corresponding

Fig. 1 (Colour online)
a Optode image (grey scale images converted to false colour) of oxygen distribution in sediments and in an *H. diversicolor* burrow and location of the zones investigated during the study (burrow zones: A1–A5; surface: S; overlying water: OW). Hatched zone: part of the burrow lumen that could not be observed because it was occupied by the worm; arrows direction of water flow during ventilation.
b Example of areas (P1–P6) selected for the extraction of oxygen profiles for diffusive oxygen flux calculation.
c, d examples of full recorded optode images of oxygen distribution in periods of low and high water oxygen concentration in the burrow, respectively



236 oxygen concentration. For full details of the experi-
 237 mental set-up, see Pischedda et al. (2008). In brief, the
 238 optode was excited by a Xenon lamp light (Perkin
 239 Elmer, 300 Watts) passing through a shutter and an
 240 excitation glass filter (405 ± 10 nm, Omega Optical)
 241 mounted on a first filter wheel. Light emitted by the
 242 optode sensing membrane was collected through a

243 Nikon macro lens and an emission glass filter
 244 (654 ± 24 nm) mounted on a second filter wheel.
 245 The fluorescence signal was then detected by a Peltier-
 246 cooled 12-bit monochrome CCD camera (KAI 2000,
 247 $1,600 \times 1,200$ pixels, 7.4×7.4 μm). Images were
 248 taken in darkness with an integration time of 30 s for
 249 oxygen and of 1 s for the sediment structure (without

any filter). The light shutter, excitation and emission filter wheels and camera were computer-controlled using the Image Pro Plus—Scope Pro package installed on a Pentium 4 computer. The digital TIFF images were then stored using 12-bit grey scale (0–4,095). The acquisition and storage of oxygen images were automated with a custom-made script.

Image processing

A non-linear relationship slightly modified from the Stern–Volmer equation (Klimant et al., 1995) was used to convert the pixel intensity (arbitrary units) into oxygen concentration as follows:

$$I = I_0[\alpha + (1 - \alpha)(1/1 + K_{sv}C)]$$

where I_0 is the fluorescence intensity in the absence of oxygen, C is the oxygen concentration ($\mu\text{mol/l}$), K_{sv} is the quenching constant expressing the quenching efficiency (M^{-1}) and α is the non-quenchable fraction of the luminescence including scattered stray light. The constants α and K_{sv} were determined from I_0 and the two intermediate calibration points, with oxygen concentrations C_1 and C_2 corresponding to intensities I_1 and I_2 , respectively, and integrated into the following equations:

$$K_{sv} = [I_0(C_2 - C_1) - (I_1C_2 - I_2C_1)] / [(I_1 - I_2)C_1C_2]$$

$$\alpha = [I_1(1 + K_{sv}C_1) - I_0] / (I_0K_{sv}C_1)$$

α and K_{sv} were averaged for each zone studied taking into account the closest anoxic zone. Having estimated α , K_{sv} and I_0 , the oxygen concentration was obtained by rearranging the first equation:

$$C = (I_0 - I) / (K_{sv}(I - I_0\alpha))$$

Due to the problems we have already mentioned, the oxygen optode was calibrated specifically for each zone studied. Table 1 shows the variation in the constants K_{sv} and α calculated from data extracted within a 50×50 pixel area. K_{sv} ranged from $20.6 \pm 2.6 \times 10^{-3} \text{ M}^{-1}$ (A3, mean \pm SD, $N = 2,500$) to $26.8 \pm 2.9 \times 10^{-3} \text{ M}^{-1}$ (A5, mean \pm SD, $N = 2,500$), which corresponded to a maximum of 13% variation from the mean value, $23.7 \pm 2.4 \times 10^{-3} \text{ M}^{-1}$ (mean \pm SD, $N = 2,500$). The variation in K_{sv} induced a variation in α of 0.7% around the mean value, $77.1 \pm 0.4 \times 10^{-2}$ (mean \pm SD, $N = 2,500$). Based on the mean

constants, the oxygen value corresponding to an intensity of 88.6 (arbitrary unit) was $190.5 \mu\text{mol l}^{-1}$, which may have varied by up to 2.3% depending on the zone considered, with a global calibration. This confirms that the differences in the K_{sv} values did indeed have a significant effect on oxygen concentration values, but this was limited by the separate calibration of the oxygen optode for each of the zones studied.

Vertical oxygen profiles extracted from 2D oxygen measurements were used to determine diffusive oxygen fluxes ($J_{(z)}$, $\text{mmol m}^{-2} \text{ d}^{-1}$), which were calculated from Fick's first law of diffusion, based on the assumption that molecular diffusion was the main oxygen transport mechanism involved (Berner, 1980; Jørgensen & Revsbech, 1985; Rasmussen & Jørgensen, 1992):

$$J_{(z)} = -\Phi D_s \partial C_{(z)} / \partial z$$

where Φ is the porosity (0.69), C is the oxygen concentration ($\mu\text{mol l}^{-1}$), z is the depth of oxygen penetration into sediments (cm) and $\partial C_{(z)} / \partial z$ is the oxygen gradient. D_s is the oxygen diffusion coefficient in sediments ($1.24 \times 10^{-5} \text{ cm}^2 \text{ s}^{-1}$), which was calculated on the basis of the following relationship (Berner, 1980): $D_s = D_0 / \theta^2$, where θ is the tortuosity and D_0 is the diffusion coefficient of oxygen in water ($\text{cm}^2 \text{ d}^{-1}$). Finally θ^2 may be estimated from the following equation (Boudreau, 1996): $\theta^2 = 1 - \ln(\Phi^2)$.

Because the data set was composed of numerous images ($N = 121$, image size: $9.3 \times 3.7 \text{ cm}$, pixel size: $800 \times 800 \mu\text{m}$), they were processed using MatLab[®] software, which applied the required procedure successively to the 121 images. A low-pass filter (3×3 pixels) was applied to the raw images and the pixel fluorescence intensity was converted into oxygen concentration. The MatLab[®] script made it possible to extract the oxygen concentration in each of the zones studied (Fig. 1a). Oxygen concentration was averaged for each zone in the 121 images. In order to measure the oxygen penetration and calculate the oxygen diffusive flux, three oxygen profiles at the sediment surface and six profiles in each burrow zone were extracted (P1, P2 and P3 on the left side of the burrow wall, and P4, P5 and P6 on the right side, Fig. 1b). Each extracted profile corresponded to six neighbouring pixel lines, which were averaged. The sediment–water interface at the surface and in the burrow was

Table 1 Coefficients K_{sv} and α calculated from data extracted within a 50×50 pixels area ($N = 2,500$), for each zone of the *H. diversicolor* burrow studied (surface and A1–A5)

Zone	K_{sv} (10^{-3} M^{-1})		α (10^{-2})		O_2 $\mu\text{mol/l}$
	Mean	SD	Mean	SD	
Surface	26.9	3	77.7	0.4	194.1
A1	22.7	3.5	76.9	0.6	188.0
A2	22.1	2.2	76.9	0.4	193.1
A3	20.6	2.6	76.6	0.6	193.9
A4	22.9	2.3	77	0.4	190.8
A5	26.8	2.9	77.7	0.4	194.8
Mean value (\pm SD)	23.7 \pm 2.4		77.1 \pm 0.4		190.5

339 located manually on corresponding greyscale images.
 340 Another custom-made MatLab[®] script allowed the
 341 oxygen gradient at the sediment–water interface to be
 342 calculated, in order to calculate the diffusive flux. The
 343 depth to which oxygen penetrated into the sediment
 344 was located automatically and for each oxygen profile,
 345 was taken to be the depth where the oxygen value
 346 dropped below $1 \mu\text{mol l}^{-1}$.

347 Statistical analyses

348 Statistical comparisons between time series of oxygen
 349 concentration, flux and penetration data in the zones
 350 studied were performed with a non-parametric Fried-
 351 man test (121 observations for each of the 6 samples,
 352 i.e. the zones studied). When a significant difference
 353 was observed between samples (5% tolerance), a
 354 multiple paired comparison was performed following
 355 the Nemenyi procedure (bilateral test). Linear regres-
 356 sions between temporal series were performed with
 357 the correlation matrix of Pearson (5% tolerance). The
 358 time-lag between the time series was determined on
 359 the basis of the better linear regression obtained by
 360 progressively shifting one temporal series with respect
 361 to another. The symmetry between the oxygenation of
 362 the right and the left part of the zones studied in the
 363 burrows was evaluated by an asymmetry index (S),
 364 which was calculated by integrating their differences.
 365 The integral was calculated on the basis of the
 366 Riemann method, corresponding to the sum of the
 367 squared differences between the right and left parts in
 368 each zone, multiplied by the interval of the measure-
 369 ment. The result was then divided by 10 to obtain the
 370 asymmetry index AS. The greater the value of AS, the
 371 more asymmetric the samples.

Results

Visual observations of the burrows

Unfortunately, only one of the *H. diversicolor* spec-
 imens constructed a U-shaped burrow (approximately
 8 cm deep) that was completely adjacent to a side of
 the tank and therefore clearly visible. The lumen of
 this burrow was visible almost in entirety, except for
 one small area in the bottom part where the worm was
 located (Fig. 1a). Most of the sediment was greyish-
 brown, indicating that it was reduced, except for a
 light-brown layer a few millimetres thick of oxidised
 sediment along the burrow wall and at the surface.
 During the experiment, we observed that the worm
 stayed in the bottom part of the burrow with its head
 facing towards the right side. The ventilation was
 unidirectional and water circulated from the worm's
 head to tail, i.e. water entered from the inhalant
 opening zone A1 and left the burrow via the exhalant
 opening zone A5.

Burrow oxygen concentrations

Burrow structures extended the oxic sediment–water
 interface, allowing oxygen to penetrate deep into the
 anoxic sedimentary column (Fig. 1c, d). The oxygen
 concentration in overlying water varied between 126.0
 and $146.0 \mu\text{mol l}^{-1}$, with a mean of 133.1 ± 3.5
 $\mu\text{mol l}^{-1}$ (mean \pm SD, $N = 121$, Fig. 2). One should
 note that these mean oxygen values were low because
 of the stratification of the tank water column in the
 absence of water mixing. Oxygen values of around
 $200 \mu\text{M}$ were measured (data not shown) in the upper
 part of the water column where the system was
 aerated, but the oxygen level decreased as it
 approached the sediment due to oxygen consumption

405 by the sediment. The area used to calculate the mean
 406 oxygen concentration of the overlying water was
 407 principally positioned close to the sediment, and
 408 therefore gave low mean values. During the experi-
 409 ment, the oxygen concentration recorded in the burrow
 410 lumen varied between $27.4 \mu\text{mol l}^{-1}$ (A4) and
 411 $90.9 \mu\text{mol l}^{-1}$ (A1), with a mean value of $56.4 \pm$
 412 $15.3 \mu\text{mol l}^{-1}$ (mean \pm SD, $N = 605$, Fig. 2). The
 413 mean oxygen concentration of water passing through
 414 the burrow varied between $78.0 \pm 7.3 \mu\text{mol l}^{-1}$ (A1,
 415 mean \pm SD, $N = 605$) and $42.3 \pm 8.0 \mu\text{mol l}^{-1}$ (A4,
 416 mean \pm SD, $N = 605$). Oxygen concentration
 417 decreased from the burrow inhalant opening (A1) to
 418 the intermediate zone (A4), and increased slightly at
 419 the exhalant opening (A5: $58.0 \pm 4.7 \mu\text{mol l}^{-1}$,
 420 mean \pm SD, $N = 605$). It was significantly different
 421 in each zone, except for zones A3 and A4 (Fig. 2).

422 During the experiment, oxygen concentration con-
 423 tinuously fluctuated in the burrow lumen (Fig. 3). The
 424 amplitude of these fluctuations was most pronounced
 425 in the intermediate and bottom zones A2 and A3,
 426 respectively (Fig. 2). The change in oxygen concentra-
 427 tion over time in neighbouring zones, such as A2
 428 and A3 (linear regression, $R^2 = 0.38$) or A3 and A4
 429 ($R^2 = 0.36$), was small compared with that between
 430 more distant zones such as A1 and A4 ($R^2 = 0.05$) or
 431 A2 and A4 ($R^2 = 0.02$).

432 Oxygenation of the burrow wall

433 During the experiment, the distance to which oxygen
 434 penetrated into the sediment ranged from 1.67 to

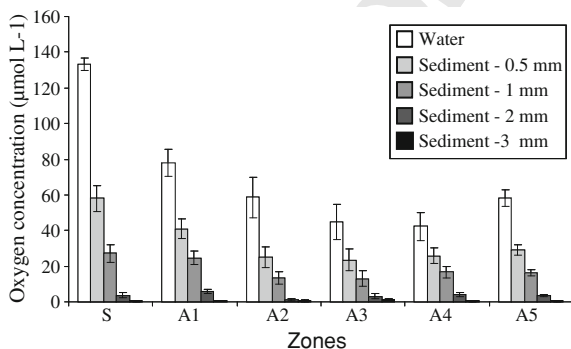


Fig. 2 Mean oxygen concentrations in free water and sedi-
 ments (0.5–3 mm distance from the interface) into the overlying
 water and the *H. diversicolor* burrow (OW and zones A1–A5,
 respectively). Error bars represent the standard deviation (SD)
 for $N = 121$

3.27 mm at the surface, with a mean value of
 2.57 ± 0.24 mm (mean \pm SD, $N = 363$), and from
 0.48 to 3.27 mm in the burrow wall, with the mean
 value varying in the different zones (Fig. 4). Oxygen
 penetrated least deeply in zones A2 (1.91 ± 0.46 mm,
 mean \pm SD, $N = 726$) and A3 (1.82 ± 0.67 mm,
 mean \pm SD, $N = 726$), whereas it penetrated most
 deeply in zone A1 (2.62 ± 0.29 mm, mean \pm SD,
 $N = 726$). Each zone had an oxygen penetration
 distance that differed significantly from that of the
 other zones, except zones A4 and A5 (Fig. 4).

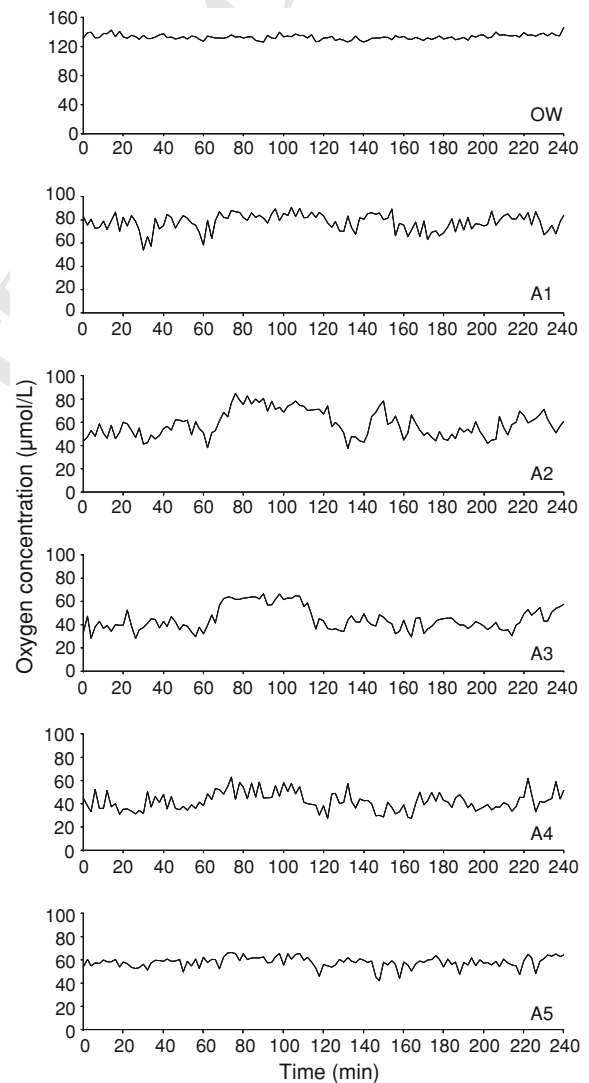


Fig. 3 Dynamics of the oxygen concentration in overlying
 water (OW) and in the *H. diversicolor* burrow lumen (zones
 A1–A5) during the experiment

446 Within the burrow wall, oxygen concentration was
 447 monitored up to 3 mm from the lumen. For each zone,
 448 the mean oxygen concentration decreased with
 449 increasing distance from the lumen (Fig. 2). The wall
 450 oxygen concentration was 43–61, 23–40, 1–7 and
 451 <2% of the lumen concentration at 0.5, 1, 2 and 3 mm
 452 distances from the lumen, respectively. Despite these
 453 lower concentrations, the oxygen dynamics presented
 454 a similar pattern to those in the lumen, at least as far as
 455 1 mm into the wall, with oxygen concentration
 456 decreasing from the inhalant opening towards the
 457 bottom, and then slightly increasing up to the exhalant
 458 opening A5 (Fig. 2). From a temporal point of view, as
 459 illustrated for the bottom zone of the burrow (A3,
 460 Fig. 5), oxygen fluctuations were also detected within
 461 the wall, but with lower amplitudes. The best linear
 462 correlations were obtained with a time-lag of zero

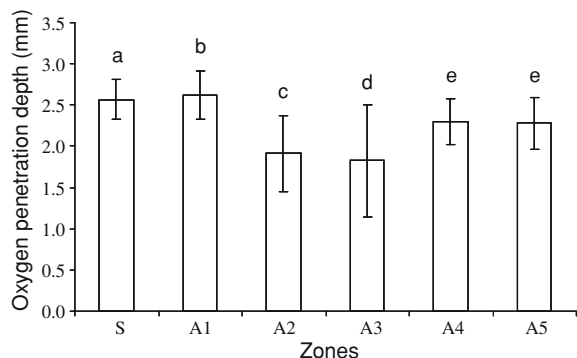
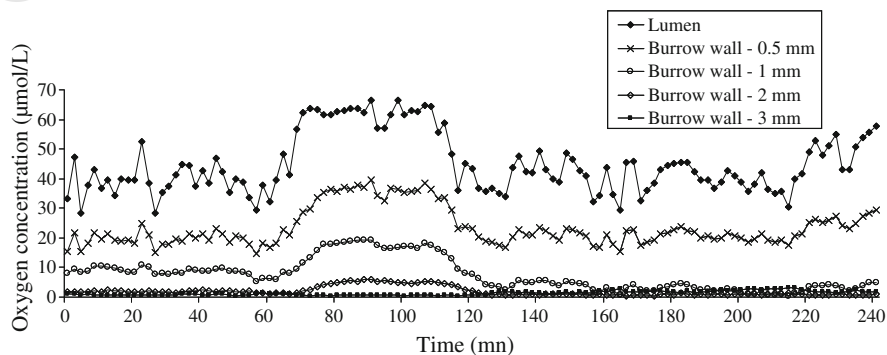


Fig. 4 Mean oxygen penetration depth at the sediment surface and in the wall of the *H. diversicolor* burrow (zones A1–A5). Error bars represent the standard deviation (SD) for $N = 363$ (surface) and $n = 726$ (burrow). Letters *a*, *b*, *c*, *d* and *e* correspond to significant differences between the zones studied (non-parametric Friedman test, 5% tolerance significance level, and multiple paired comparisons following the bilateral test, Nemenyi procedure)

Fig. 5 Oxygen dynamics in the lumen and wall of the *H. diversicolor* burrow (0.5–3 mm distance from the lumen) in the bottom zone A3. Values are the means of the six profiles in each zone



($R^2 = 0.91$), 2 ($R^2 = 0.82$) and 6 min ($R^2 = 0.72$) at 463
 464 0.5, 1 and 2 mm, respectively.

465 Looking more precisely at oxygen penetration into
 466 the burrow wall, and more especially at the duration of
 467 oxygenation (i.e. the time during which some oxygen
 468 is present as a percentage of the total duration of the
 469 experiment) in the first few millimetres of the right and
 470 left parts of the burrow, a radial dissymmetry based on
 471 the oxygenation level was detected in each zone
 472 (Fig. 6). The bottom zone (A3) and the exhalant
 473 opening zone (A5) appeared to display the greatest
 474 asymmetry (i.e. the greatest difference between the
 475 left and right parts of the burrow), estimated by
 476 asymmetry indices, AS, of 315 and 333, respectively.
 477 Zones A2 (AS = 56) and A4 (AS = 48) presented
 478 intermediate asymmetries, and the inhalant opening
 479 zone (A1) was the most symmetrical (AS = 3).

480 The area of oxygenated sediments observable on the
 481 oxygen images was on average $8.4 \pm 0.8 \text{ cm}^2$ (mean \pm
 482 SD, $N = 121$), 87% of which was due to the presence
 483 of the burrow. Moreover, if we consider the burrow
 484 itself, the mean surface of oxygenated sediment was
 485 $7.3 \pm 0.8 \text{ cm}^2$ (mean \pm SD, $N = 121$); this was 20%
 486 higher during the active periods of worm ventilation
 487 activity and 20% lower during the rest periods.

Oxygen diffusive flux

488
 489 The diffusive flux of oxygen at the surface ranged
 490 from 1.4 to $12.7 \text{ mmol m}^{-2} \text{ d}^{-1}$, with a mean of
 491 $6.50 \pm 1.46 \text{ mmol m}^{-2} \text{ d}^{-1}$ (mean \pm SD, $N = 363$),
 492 whereas the flux across the burrow wall ranged from
 493 0.7 to $6.6 \text{ mmol m}^{-2} \text{ d}^{-1}$ (Fig. 7). Like the mean
 494 oxygen distribution in the burrow lumen, the mean
 495 diffusive flux decreased from the inhalant opening
 496 zone (A1, $4.07 \pm 1.01 \text{ mmol m}^{-2} \text{ d}^{-1}$, mean \pm SD,
 497 $N = 726$) towards the intermediate zone A4 ($1.92 \pm$

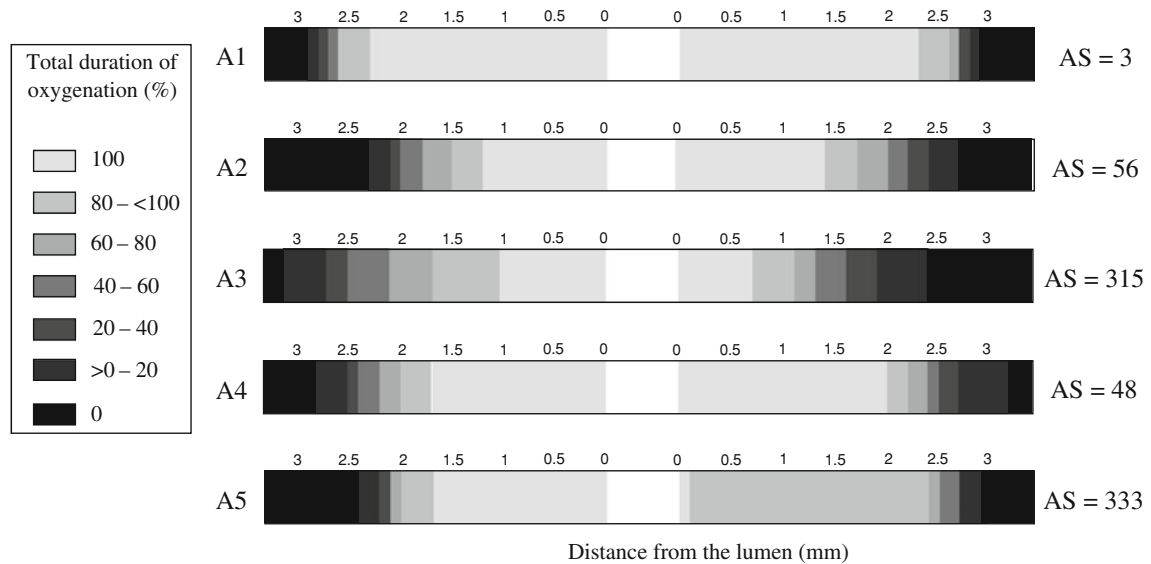


Fig. 6 Duration of oxygenation (i.e. the time during which some oxygen is present as a percentage of the total duration of the experiment) in the first few millimetres of the right and left

parts of the burrow, for zones A1–A5. The symmetry between the oxygenation of the right and the left sides is quantified by the asymmetry index (AS) (see text)

498 $0.49 \text{ mmol m}^{-2} \text{ d}^{-1}$, mean \pm SD, $N = 726$), and
 499 then increased slightly at the exhalant opening (A5,
 500 $2.48 \pm 0.69 \text{ mmol m}^{-2} \text{ d}^{-1}$, mean \pm SD, $N = 726$).
 501 Fluxes exhibited high variability, especially at the
 502 surface, in the inhalant opening zone (A1) and in the
 503 intermediate zone located immediately beneath it (A2,
 504 $3.65 \pm 0.80 \text{ mmol m}^{-2} \text{ d}^{-1}$, mean \pm SD, $N = 726$).
 505 The oxygen diffusive flux values were all significantly
 506 different, except between zones A1 and A2 and
 507 between zones A3 and A5 (Fig. 7).

508 Oxygen penetration and diffusive flux within the
 509 burrow wall both exhibited the same temporal pattern
 510 as those in the lumen. As illustrated by Fig. 8 for the
 511 bottom zone (A3), both varied in accordance with the
 512 concentrations of oxygen in the water, with a time-lag
 513 of about 4 min for the oxygen penetration depth
 514 ($R^2 = 0.47$), and with no time-lag for the diffusive
 515 flux ($R^2 = 0.38$).

516 Discussion

517 Oxygen fluctuations in the *H. diversicolor* burrow

518 Previous studies that specifically monitored the macro-
 519 faunal ventilation cycle were based on measuring water
 520 flow rather than on directly measuring oxygen levels

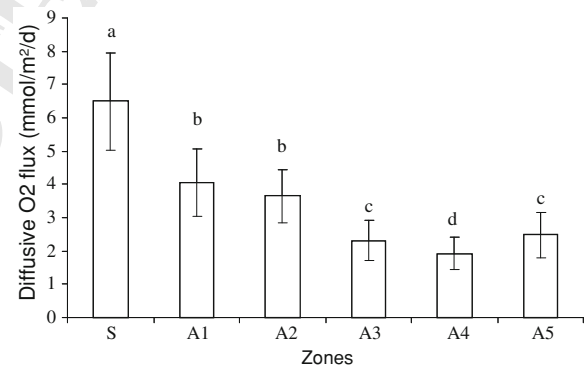
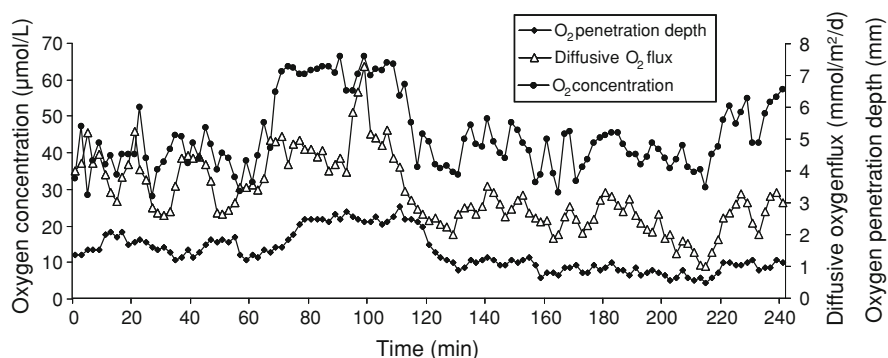


Fig. 7 Mean diffusive oxygen fluxes at the surface and in the *H. diversicolor* burrow (zones A1–A5). Error bars represent the standard deviation (SD) for $N = 363$ (surface) and $n = 726$ (burrow). Letters a, b, c and d correspond to significant differences between the zones studied (non-parametric Friedman test, 5% tolerance significance level, and multiple paired comparison following the bilateral test, Nemenyi procedure)

521 within the burrow (for a review, see Riisgard & Larsen, 521
 522 2005). Specific studies of *H. diversicolor* have shown 522
 523 that this species intermittently ventilates its burrow 523
 524 following a regular cycle of active (~ 10 min) and 524
 525 resting phases (~ 5 min) (e.g. Kristensen, 1981). No 525
 526 clear ventilation pattern was detected in the burrow 526
 527 lumen in this study, mainly because of the method of 527
 528 data acquisition, where each oxygen picture represented 528

Fig. 8 Dynamics of the oxygen concentration in the lumen, the diffusive oxygen flux and the depth to which oxygen penetrated in the *H. diversicolor* burrow wall, in the bottom zone (A3)



529 an event lasting 30 s, which corresponded to the time
530 required for image acquisition. Moreover, the interval
531 between two measurements was 2 min, which limited
532 our ability to assess the worm ventilation cycle within
533 the burrow. However, our results do show that oxygen
534 concentration fluctuated at a scale of minutes in the
535 burrow, and we can reasonably link this to worm
536 ventilation activity. A similar pattern was detected
537 within the burrow wall, where oxygen concentrations
538 reflected those in the lumen, as previously reported for
539 other ventilating species such as the polychaetes
540 *A. marina* (Timmermann et al., 2006) and *Lanice*
541 *conchilega*, and the crustacean *Callianassa subterranea*
542 (Forster & Graf, 1995). However, while we observed
543 decreasing amplitudes of oxygen fluctuations in correlation
544 with increasing distance from the lumen, we also
545 observed an increasing time-lag in the oxygen dynamics
546 in the lumen. The latter, which was related to patterns of
547 change in both oxygen penetration depth and diffusive
548 flux, was clearly dependent on the time taken for oxygen
549 to diffuse from the lumen to the wall.

550 Increases in oxygen concentration and penetration
551 into the burrow wall were closely associated with
552 active macrofaunal ventilation. We were able to
553 distinguish three micro-horizons in the burrow wall,
554 presumably resulting from intermittent worm bio-
555 irrigation: a permanently oxic layer, a layer oscillating
556 between oxic and anoxic conditions and, at a distance
557 too far from the burrow lumen to allow oxygen to
558 penetrate, a permanently anoxic layer ($O_2 < 1$
559 $\mu\text{mol l}^{-1}$ in this study). The two first layers corre-
560 sponded to a thickness that was spatially variable
561 within the structure and highly dynamic ($\pm 20\%$)
562 following the worm ventilation pattern. This oxygen
563 zoning is of major importance, since it has been shown
564 that rates and pathways of organic matter degradation
565 are not the same under oxic, anoxic and oscillating

566 redox conditions (Sun et al., 2002). In fact, organic
567 matter degradation can occur up to ten times as fast
568 under oxic as under anoxic conditions (Kristensen,
569 2000). Furthermore, redox oscillations are accom-
570 panied by rapid switches in the dominant bacterial
571 metabolism, influencing both organic matter burial
572 and geochemical cycles (Hansen & Kristensen, 1998;
573 Rosenberg, 2001). For instance, Caradec et al. (2004)
574 found that the continuous or a periodic presence of
575 oxygen stimulated the degradation of some lipids
576 (triacylglycerols) and the subsequent degradation of
577 the metabolites released (e.g. free fatty acids), leading
578 to lower residual concentrations of such lipids in the
579 sediment than under anoxic conditions.

Oxygen spatial heterogeneity

580
581 In this study, the burrow exhibited significantly lower
582 oxygen concentrations than the overlying water. The
583 maximum oxygen concentration in the burrow lumen,
584 observed in the most highly oxygenated zone (i.e. the
585 inhalant opening zone A1) was only 70% of the mean
586 oxygen concentration in overlying water ($133.1 \pm$
587 $3.5 \mu\text{mol l}^{-1}$). In addition, the composition of the
588 burrow water did not remain identical to that of the
589 overlying water during ventilation. Indeed, the volume
590 of water replaced by each pumping of the macrofauna
591 is smaller than the volume of the burrow cavity, and
592 the velocity of water due to macrofauna flushing has a
593 finite value (Aller et al., 1983; Kristensen et al., 1991).
594 The low concentration of oxygen in the burrow
595 demonstrates that *H. diversicolor* can live without
596 highly oxygenated water, as already suggested by its
597 high ecological tolerance of sulphide (Vismann,
598 1990). Under unfavourable environmental conditions,
599 such as low oxygen concentration, *H. diversicolor* is
600 able to regulate oxygen uptake by a combination of

601 behavioural and physiological mechanisms (e.g. an
602 increase in ventilation activity, the optimisation of
603 oxygen extraction; Kristensen, 1983). It is also able to
604 switch to extended anaerobiosis during persistent
605 anoxia or excessive levels of sulphide (Schottler,
606 1979; Jahn et al., 1992).

607 The *H. diversicolor* burrow displayed a heteroge-
608 neous distribution of oxygen, as shown by the
609 decreasing trend from the inhalant opening down to
610 the burrow bottom, and then a slight increase up to the
611 exhalant opening. This reflects the progressive con-
612 sumption of oxygen as water circulates within the
613 burrow lumen during active ventilation. In fact,
614 burrow oxygen is consumed by both worm and
615 microbe respiration and by re-oxidation of inorganic
616 metabolites produced by anaerobic metabolisms in
617 surrounding sediments (Jørgensen, 1983). Although
618 the fauna is important for the benthic oxygen uptake,
619 faunal respiration itself constitutes only a minor part of
620 the total fauna-related oxygen consumption, as dem-
621 onstrated by experimental and in situ measurements
622 (e.g. Kristensen, 1985; Glud et al., 2003; Dunn et al.,
623 2009; Paspasyrou et al., 2010).

624 The above discussion is based on the assumption
625 that the burrow constitutes a homogeneous structure,
626 which both the inter- and intra-zone (asymmetry)
627 comparisons reported here indicate is clearly not the
628 case. Despite the initial homogenisation of the sedi-
629 mentary matrix before the experiment, the surround-
630 ing sediments, and the burrow wall in particular, may
631 give rise to patchiness. For example, mucous secre-
632 tions may have been irregularly distributed along the
633 burrow wall, influencing (1) the local intensity of
634 microbial reactions, since the mucus layer is com-
635 posed of labile organic substances and (2) the local
636 thickness of the layer through which oxygen may
637 diffuse, even if the mucus layer is not considered to be
638 a barrier to oxygen diffusion (Aller, 1988; Fenchel,
639 1996; Hannides et al., 2005). We also observed that
640 the amplitude of oxygen fluctuations was less pro-
641 nounced in the upper part of the burrow than in the
642 lower part. This phenomenon is probably due to the
643 proximity of the upper zones (A1 and A5) to the oxy-
644 gen-rich overlying surface water. Surface dissolved
645 oxygen, which was present in limitless quantities in the
646 overlying water, may have been constantly diffusing
647 into these nearby upper burrow zones, resulting in a
648 'buffer effect'. Deeper down in the sediments, i.e.
649 further from the oxygen reservoir, the burrow did not

benefit from this effect and the amplitude of oxygen 650
fluctuation was therefore greater. The impact of the 651
buffer effect was observed not only in the burrow 652
lumen, but also in the burrow wall, where the radial 653
dissymmetry of oxygenation was higher in the bottom 654
zone. 655

Influence of oxygen distribution heterogeneity 656
on diffusive flux 657

Diffusive oxygen flux was calculated on the basis of the 658
profiles extracted from the oxygen images. However, 659
as emphasised by Glud et al. (1996), the wall effect of 660
the tank induces distortion of the diffusive boundary 661
layer (DBL), which makes simple calculations of the 662
diffusive flux based on DBL-based data less meaning- 663
ful. Nevertheless, we considered that the calculated 664
fluxes could be used as comparative data in this study. 665
Diffusive oxygen fluxes within the burrow wall were 666
on average 1.5–3.5 times lower than those in the 667
surface sediments. In a similar experiment, Pischedda 668
et al. (2008) found equivalent or lower diffusive 669
oxygen fluxes in the *H. diversicolor* burrow compared 670
with surface sediments. The oxygen concentration in 671
the burrow could explain these lower fluxes. Our 672
results showed that diffusive fluxes in the burrow were 673
directly influenced by the oxygen concentration in the 674
lumen, since they followed the same spatial and 675
temporal pattern. For example, when oxygen concen- 676
tration increased within the lumen, it diffused in a 677
radial pattern towards the burrow wall, generating a 678
steeper gradient at the sediment–water interface and 679
resulting in a higher flux. Therefore, it is reasonable to 680
assume that fluxes in the burrow were lower than those 681
in the surface because of the lower oxygen concentra- 682
tion in the burrow. Moreover, some of the oxygen 683
consumed within the burrows is used for the chemical 684
and biological reoxydation of reduced compounds (e.g. 685
iron (II) and sulphide). Two-dimensional zonations of 686
these reduced compounds have been shown to be 687
highly heterogeneous in bioturbated sediments, 688
particularly in the vicinity of burrows and roots 689
(Robertson et al., 2009; Bertics et al., 2010; Bertics & 690
Ziebis, 2010; Pagès et al., 2011), which could poten- 691
tially drive variable fluxes of both reduced compounds 692
and oxygen in the different part of the burrows. 693

Differences between diffusive fluxes at the surface 694
and in the burrow are also likely to be linked to the 695
microbial nature of the sedimentary matrix. The 696

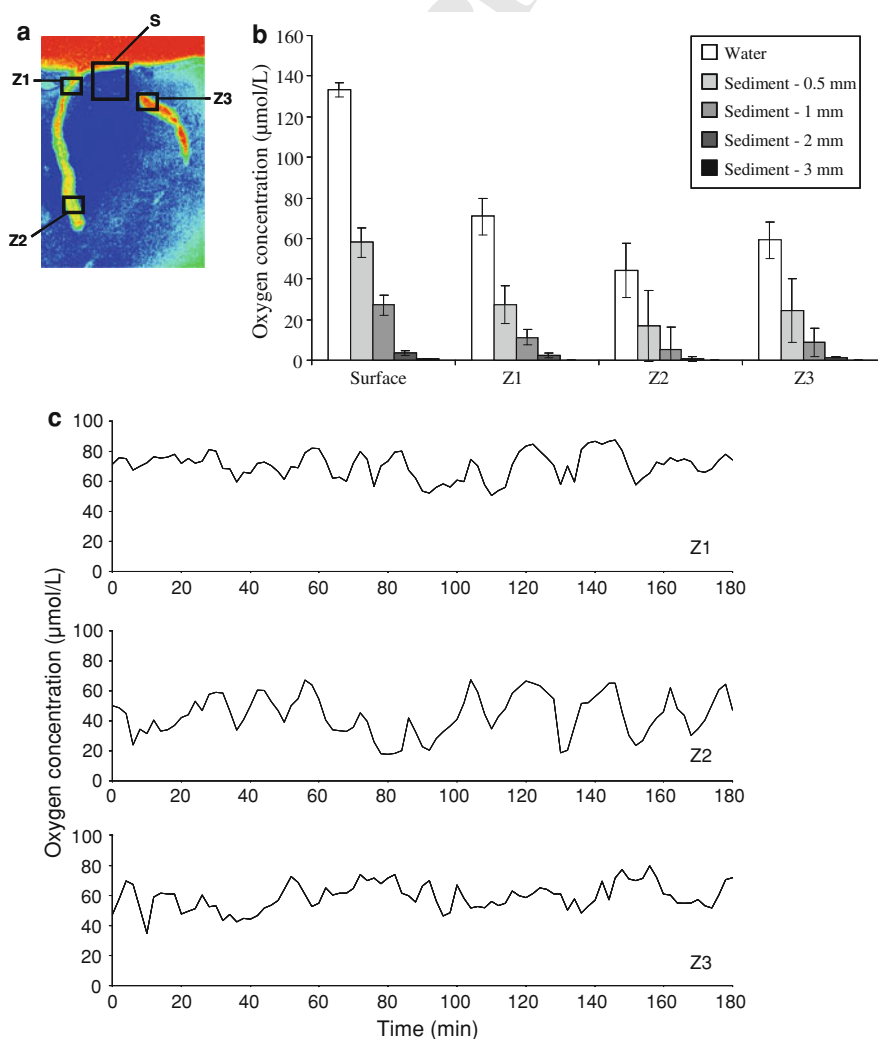
697 burrow structure is not simply an extension of the
698 sediment surface, but has unique physical–chemical
699 properties and microbial community characteristics
700 that may indirectly influence oxygen uptake (Aller &
701 Aller, 1986; Papaspyrou et al., 2005). Burrow walls
702 have been shown to be microbial degradation hotspots,
703 presenting different bacterial assemblages and higher
704 bacterial abundance and activity rates than surface
705 sediments (e.g. Marinelli et al., 2002; Papaspyrou
706 et al., 2006). These differences could be linked to the
707 mucus lining, which directly enriches the burrow wall
708 with labile organic matter, but can also act as a trap for
709 phytoplankton (Defretin, 1971; Kristensen, 2000).

A representative and ‘typical’ burrow?

710

This study was based on a single *H. diversicolor*
711 burrow. Indeed, only one individual produced a
712 complete structure during the experiment. However,
713 we also looked at another randomly chosen burrow
714 (Fig. 9a), and found that despite its incomplete
715 structure, it displayed similar oxygen dynamics and
716 distribution features, e.g. burrow oxygen dynamics
717 were linked to the lumen oxygen pattern (Fig. 9b), and
718 the oxygen concentration was lower but the oxygen
719 fluctuation higher in the burrow lumen in the deeper
720 zone, Z2 (Z1: $70.7 \pm 8.8 \mu\text{mol l}^{-1}$; Z2: 44.2 ± 13.6
721

Fig. 9 (Colour online)
a Optode image (grey scale images were converted to false colour) of oxygen distribution in sediments and in the *H. diversicolor* burrow and location of the zones investigated (Burrow zones: Z1–Z3; surface: S);
b mean oxygen concentrations in free water and sediments (0.5–3 mm distance from the interface) in the overlying water and the *H. diversicolor* burrow (OW and zones Z1–Z3, respectively). Error bars represent the standard deviation (SD) for $N = 121$;
c dynamics of oxygen concentration in the *H. diversicolor* burrow lumen (zones Z1–Z3)



722 $\mu\text{mol l}^{-1}$; Z3: $59.2 \pm 8.9 \mu\text{mol l}^{-1}$; mean \pm SD,
723 $N = 455$; Fig. 9c). This allows us to consider that
724 the features demonstrated in the studied burrow can be
725 extrapolated to burrows in general.

726 Also, in order to be able to assess the representa-
727 tiveness of the *H. diversicolor* burrow we studied, we
728 have to consider how its characteristics could in fact
729 vary. The oxygen-related functioning of a burrow can
730 be modified by:

- 731 – the bio-irrigation pattern of *H. diversicolor* that
732 can change depending on the worm feeding
733 strategy—deposit-feeding, filter-feeding, herbi-
734 vore or carnivore (Esnault et al., 1990; Riisgard,
735 1991)—which is linked to food availability and
736 quality, the presence or absence of predators, the
737 tidal height and season (Esselink & Zwarts, 1989;
738 Masson et al., 1995), and the water temperature
739 (Gerino, 1989);
- 740 – the age of the burrow, which could potentially
741 modify the local hydrodynamics due to the
742 increased complexity of galleries' system (Davey,
743 1994) and also affect the bacterial structure within
744 the burrow (Marinelli et al., 2002).

745 Such differences in oxygen supply, in burrow
746 microstructure and in the microbial communities
747 living within the burrow microenvironment would
748 modify the oxygen content and the diffusive properties
749 of the burrow wall. An in situ study by Wenzhöfer &
750 Glud (2004) in a shallow environment dominated by *H.*
751 *diversicolor* also documented a highly dynamic distri-
752 bution of oxygen in the burrow wall, which varied with
753 time on a diel scale and with the environmental
754 conditions. Thus, the data obtained in this study can be
755 considered to be representative of what can happen to
756 oxygen fluxes and distribution, under the specific
757 conditions in the burrow of a specimen of this species.

758 Conclusion

759 This study shows that oxygen is heterogeneously
760 distributed in the lumen and wall of an *H. diversicolor*
761 burrow. More specifically, the properties (size and
762 duration of oxygenation) of the three micro-horizons
763 surrounding the burrow lumen (oxic, oscillating and
764 anoxic) are spatially and temporally variable within
765 the structure. The distribution of oxygen within the
766 burrow seems to be controlled by (i) the distance from

the sediment–water interface and (ii) the direction of
water circulation resulting from active ventilation.
Moreover, in the upper part of the structure, a ‘buffer
effect’, induced by the proximity of the overlying
water, reduces the variations in oxygen levels in the
burrow lumen and wall. These findings about the
depth-dependence and temporal variation of oxygen
concentration add substantially to our understanding
of *H. diversicolor* burrow function. In doing so, it goes
some way towards meeting the requirement formu-
lated by Koretsky et al. (2002) for the development of
ecology-based bio-irrigation models necessary to
estimate the ecological importance of burrowing
species in coastal ecosystems.

Acknowledgments This study is part of Laura Pischedda's
PhD research. The study was supported by the EU Commission
(STREP COBO; contract number GOCE-CT-2003-505564) and
the French programme ANR DHYVA (project ANR-06-SEST-
09). We thank Dr. David Nerini and Dr. Matthias Gauduchon for
constructive discussions and advice on the statistics and the flux
calculation. Thanks are also due to the anonymous reviewers for
thoughtful comments which improved the original manuscript.
Nereis Park contribution number 28.

References

- Aller, R. C., 1980. Quantifying solute distribution in the bio-
turbated zone of marine sediments by defining an average
microenvironment. *Geochimica et Cosmochimica Acta* 44:
1955–1965.
- Aller, R. C., 1988. Benthic fauna and biogeochemical processes
in marine sediments: the role of burrow structures. In
Blackburn, T. H. & J. Sorensen (eds), *Nitrogen Cycling in
Coastal Marine Environments*. Wiley, Chichester:
301–338.
- Aller, R. C., 1994. Bioturbation and remineralization of sedi-
mentary organic matter: effects of redox oscillation.
Chemical Geology 114: 331–345.
- Aller, R. C., 2001. Transport and reactions in the bioirrigated
zone. In Boudreau, B. P. & B. B. Jørgensen (eds), *The
Benthic Boundary Layer: Transport processes and
Biogeochemistry*. Oxford Press, Oxford: 269–301.
- Aller, J. Y. & R. C. Aller, 1986. Evidence for localized
enhancement of biological activity associated with tube
and burrow structures in deep sea sediments at the Hebble
site, Western North-Atlantic. *Deep-Sea Research Part
A—Oceanography Research Papers* 33: 755–790.
- Aller, R. C., J. Y. Yingst & W. J. Ullman, 1983. Comparative
biogeochemistry of water in intertidal *Onuphis* (polycha-
eta) and *Upogebia* (crustacean) burrows—temporal pattern
and causes. *Journal of Marine Research* 41(3): 571–604.
- Anderson, J. G. & P. S. Meadows, 1978. Microenvironments in
marine sediments. *Proceeding of the Royal Society of
Edinburgh, Section B* 76: 1–16.

- 819 Bartels-Hardege, H. D. & E. Zeeck, 1990. Reproductive
820 behavior of *Nereis diversicolor* (Annelida, Polychaeta).
821 Marine Biology 106(3): 409–412.
- 822 Behrens, J. W., H. J. Stahl, J. F. Steffensen & R. N. Glud, 2007.
823 Oxygen dynamics around buried lesser sandeels *Ammodytes
824 tobianus* (Linnaeus 1785): mode of ventilation and
825 oxygen requirements. Journal of Experimental Biology
826 210: 1006–1014.
- 827 Berner, R. A., 1980. Early Diagenesis: A Theoretical Approach.
828 Princeton University Press, Princeton, NJ
- 829 Bertics, V. J. & W. Ziebis, 2010. Bioturbation and the role of
830 microniches for sulfate reduction in coastal marine sedi-
831 ments. Environmental Microbiology 12: 3022–3034.
- 832 Bertics, V. J., J. A. Sohm, T. Treude, C. E. Chow, D. G. Capone,
833 J. A. Fuhrman & W. Ziebis, 2010. Burrowing deeper into
834 benthic nitrogen cycling: the impact of bioturbation on
835 nitrogen fixation coupled to sulfate reduction. Marine
836 Ecology Progress Series 409: 1–15.
- 837 Boudreau, B. P., 1996. The diffusive tortuosity of fine-grained
838 un lithified sediments. Geochimica et Cosmochimica Acta
839 60(16): 3139–3142.
- 840 Boudreau, B. P. & R. L. Marinelli, 1994. A modeling study of
841 discontinuous biological irrigation. Journal of Marine
842 Research 52: 947–968.
- 843 Caradec, S., V. Grossi, F. Gilbert, C. Guigue & M. Goutx, 2004.
844 Influence of various redox conditions on the degradation of
845 microalgal triacylglycerols and fatty acids in marine sedi-
846 ments. Organic Geochemistry 35: 277–287.
- 847 Davey, J. T., 1994. The architecture of the burrow of *Nereis
848 diversicolor* and its quantification in relation to sediment-
849 water exchange. Journal of Experimental Marine Biology
850 and Ecology 179: 115–129.
- 851 Defretin, B., 1971. The tubes of polychaete annelids. In Florkin,
852 M. & E. H. Stotz (eds), Comprehensive Biochemistry.
853 Elsevier, Amsterdam: 713–747.
- 854 Dunn, R. J. K., D. T. Welsh, M. A. Jordan, P. R. Teasdale &
855 C. J. Lemckert, 2009. Influence of natural amphipod
856 (*Victoripisa australiensis*) (Chilton, 1923) population
857 densities on benthic metabolism, nutrient fluxes, denitrifi-
858 cation and DNRA in sub-tropical estuarine sediment.
859 Hydrobiologia 628: 95–109.
- 860 Dupont, E., G. Stora, P. Tremblay & F. Gilbert, 2006. Effects of
861 population density on the sediment mixing induced by the
862 gallery-diffuser *Hediste (Nereis) diversicolor* O.F. Müller,
863 1776. Journal of Experimental Marine Biology and Ecology
864 336: 33–41.
- 865 Esnault, G., C. Retière & R. Lambert, 1990. Food resource
866 partitioning in a population of *Nereis diversicolor*
867 (Annelida, Polychaeta) under experimental conditions. In
868 Proceedings of the 24th European Marine Biology Sym-
869 posium: 453–467.
- 870 Esselink, P. & L. Zwartz, 1989. Seasonal trend in burrow depth
871 and tidal variation in feeding-activity of *Nereis Diversi-
872 color*. Marine Ecology Progress Series 56(3): 243–254.
- 873 Fenchel, T., 1996. Worm burrows and oxic microniches in
874 marine sediments. I. Spatial and temporal scales. Marine
875 Biology 127: 289–295.
- 876 Forster, S. & G. Graf, 1995. Impact of irrigation on oxygen flux
877 into the sediment—intermittent pumping by *Callianassa
878 subterranea* and piston pumping by *Lanice conchilega*.
879 Marine Biology 123: 335–346.
- Foster-Smith, R. L., 1978. An analysis of water flow in tube-
living animals. Journal of Experimental Marine Biology
and Ecology 341: 73–95.
- François, F., M. Gerino, G. Stora, J. Durbec & J. C. Poggiale,
2002. Functional approach to sediment reworking by gal-
lery-forming macrobenthic organisms: modeling and
application with the polychaete *Nereis diversicolor*. Marine
Ecology Progress Series 229: 127–136.
- Furukawa, Y., 2001. Biogeochemical consequences of macro-
fauna burrow ventilation. Geochemical Transactions 2(1):
83.
- Gerino, M., 1989. Approche des processus de bioturbation : une
technique de mesure de la bio-irrigation. Journal de la
Recherche Océanographique 1–2: 24–27.
- Gilbert, F., S. Hulth, V. Grossi, J. C. Poggiale, G. Desrosiers, R.
Rosenberg, M. Gerino, F. Francois-Carcaillet, E. Michaud
& G. Stora, 2007. Sediment reworking by marine benthic
species from the Gullmar Fjord (Western Sweden):
importance of faunal biovolume. Journal of Experimental
Marine Biology and Ecology 348: 133–144.
- Gillet, P., 1993. Impact de l'implantation d'un barrage sur la
dynamique des populations de *Nereis diversicolor* (Anné-
lide polychète) de l'estuaire du Bou Regreg, Maroc. Journal
de la Recherche Océanographique 18: 15–18.
- Glud, R. N., N. B. Ramsing, J. K. Gundersen & I. Klimant, 1996.
Planar optodes: a new tool for fine scale measurements of
two-dimensional O₂ distribution in benthic communities.
Marine Ecology Progress Series 140: 217–226.
- Glud, R. N., J. K. Gundersen, H. Roy & B. B. Jørgensen, 2003.
Seasonal dynamics of benthic O₂ uptake in a semi-enclosed
bay: importance of diffusion and faunal activity. Limnol-
ogy and Oceanography 48: 1265–1276.
- Hannides, A. K. S. M., R. C. Dunn & Aller, 2005. Diffusion of
organic and inorganic solutes through macrofaunal mucus
secretions and tube linings in marine sediments. Journal of
Marine Research 63: 957–981.
- Hansen, K. & E. Kristensen, 1998. The impact of the polychaete
Nereis diversicolor and enrichment with macroalgal
(*Chaetomorpha linum*) detritus on benthic metabolism and
nutrient dynamics in organic-poor and organic-rich
sediment. Journal of Experimental Marine Biology and
Ecology 231: 201–223.
- Hulth, S., R. C. Aller, P. Engstrom & E. Selander, 2002. A pH
fluorosensor (optode) for early diagenetic studies of marine
sediments. Limnology and Oceanography 47(1): 212–220.
- Jahn, A., R. Oeschger & H. Theede, 1992. Effects of hydrogen
sulfide on the metabolism of selected polychaetes from the
North Sea and the Baltic. Verhandlungen der Deutschen
Zoologischen Gesellschaft 85(1): 22 (in German).
- Jørgensen, B. B., 1983. Processes at the sediment-water inter-
face. In Bolin, B. & R. B. Cook (eds), The Major Bio-
geochemical Cycles and Their Interactions. Scope 21,
Stockholm: 477–509.
- Jørgensen, B. B. & N. P. Revsbech, 1985. Diffusive boundary
layers and the oxygen uptake of sediments and detritus.
Limnology and Oceanography 30: 111–122.
- Kautsky, H., 1939. Quenching of luminescence by oxygen.
Transactions of the Faraday Society 35: 216–219.
- Klimant, I., V. Meyer & M. Kuhl, 1995. Fiber-optic oxygen
microsensors, a new tool in aquatic biology. Limnology
and Oceanography 40: 1159–1165.

- 941 Koretsky, C. M., C. Meile & P. Van Cappellen, 2002. Quanti- 1002
 942 fying bioirrigation using ecological parameters: a sto- 1003
 943 chastic approach. *Geochemical Transactions* 3(3): 17–33. 1004
 944 Kristensen, E., 1981. Direct measurement of ventilation and 1005
 945 oxygen uptake in 3 species of tubicolous polychaetes 1006
 946 (*Nereis* spp.). *Journal of Comparative Physiology B* 145: 1007
 947 45–50. 1008
 948 Kristensen, E., 1983. Ventilation and oxygen uptake by three 1009
 949 species of *Nereis* (Annelida, Polychaeta). 1. Effects of 1010
 950 hypoxia. *Marine Ecology Progress Series* 12: 289–297. 1011
 951 Kristensen, E., 1985. Oxygen and inorganic nitrogen exchange 1012
 952 in a *Nereis virens* (Polychaeta) bioturbated sediment water 1013
 953 system. *Journal of Coastal Research* 1: 109–116. 1014
 954 Kristensen, E., 1989. Oxygen and carbon-dioxide exchange in 1015
 955 the Polychaete *Nereis virens*—influence of ventilation 1016
 956 activity and starvation. *Marine Biology* 101(3): 381–388. 1017
 957 Kristensen, E., 2000. Organic matter diagenesis at the oxic/ 1018
 958 anoxic interface in coastal marine sediments, with 1019
 959 emphasis on the role of burrowing animals. *Hydrobiologia* 1020
 960 426(1–3): 1–24. 1021
 961 Kristensen, E., 2001. Impact of polychaetes (*Nereis* and *Aren- 1022*
 962 *icola*) on sediment biogeochemistry in coastal areas: past, 1023
 963 present, and future developments. *Abstracts of Papers of 1024*
 964 the American Chemical Society 221: U538. 1025
 965 Kristensen, E. & K. Hansen, 1999. Transport of carbon dioxide 1026
 966 and ammonium in bioturbated (*Nereis diversicolor*) coastal, 1027
 967 marine sediments. *Biogeochemistry* 45(2): 147–168. 1028
 968 Kristensen, E., M. H. Jensen & R. C. Aller, 1991. Direct mea- 1029
 969 surement of dissolved inorganic nitrogen exchange and 1030
 970 denitrification in individual polychaete (*Nereis virens*) 1031
 971 burrows. *Journal of Marine Research* 49(2): 355–377. 1032
 972 Liebsch, G., L. Klimant, B. Frank, G. Holst & O. S. Wolfbeis, 1033
 973 2000. Luminescence lifetime imaging of oxygen, pH, and 1034
 974 carbon dioxide distribution using optical sensors. *Applied 1035*
 975 Spectroscopy 54: 548–559. 1036
 976 Marinelli, R. L., C. R. Lovell, S. G. Wakeham, D. B. Ringelberg 1037
 977 & D. C. White, 2002. Experimental investigation of the 1038
 978 control of bacterial community composition in macrofa- 1039
 979unal burrows. *Marine Ecology Progress Series* 235: 1–13. 1040
 980 Masson, S., G. Desrosiers & C. Retiere, 1995. Périodicité 1041
 981 d'alimentation du polychète *Nereis virens* (OF Müller) 1042
 982 selon les changements de la Marée. *Écoscience* 2: 20–27. 1043
 983 Meile, C. & P. Van Cappellen, 2003. Global estimates of 1044
 984 enhanced solute transport in marine sediments. *Limnology 1045*
 985 and Oceanography 48: 777–786. 1046
 986 Mettam, C., 1979. Seasonal changes in populations of *Nereis 1047*
 987 *diversicolor* OF Müller from the Severn estuary UK. In 1048
 988 Nelor, E. & R. G. Hartnoll (eds), *Cyclic Phenomena in 1049*
 989 *Marine Plants and Animals*. Pergamon Press, Oxford: 1050
 990 123–130. 1051
 991 Meysman, F. J. R., O. S. Galaktionov, B. Gribsholt & J. 1052
 992 J. Middelburg, 2006. Bio-irrigation in permeable sedi- 1053
 993 ments: an assessment of model complexity. *Journal of 1054*
 994 *Marine Research* 64(4): 589–627. 1055
 995 Miron, G. & E. Kristensen, 1993. Behavioral response of three 1056
 996 nereid polychaetes to injection of sulfide inside burrows. 1057
 997 *Marine Ecology Progress Series* 101(1–2): 147–155. 1058
 998 Osovitz, C. J. & D. Julian, 2002. Burrow irrigation behavior of 1059
 999 *Urechis caupo*, a filter-feeding marine invertebrate, in its 1060
 1000 natural habitat. *Marine Ecology Progress Series* 245: 1061
 1001 149–155. 1062

- 1063 Strömberg, N., 2006. Imaging Optodes. PhD thesis, University
1064 of Göteborg, Göteborg.
- 1065 Stromberg, N. & S. Hulth, 2003. A fluorescence ratiometric
1066 detection scheme for ammonium ions based on the solvent
1067 sensitive dye MC 540. Sensors and Actuators B: Chemical
1068 90(1–3): 308–318.
- 1069 Sun, M. Y., R. C. Aller, C. Lee & S. G. Wakeham, 2002. Effects
1070 of oxygen and redox oscillation on degradation of cell-
1071 associated lipids in surficial marine sediments. Geochimi-
1072 mica et Cosmochimica Acta 66: 2003–2012.
- 1073 Timmermann, K., G. T. Banta & R. N. Glud, 2006. Linking
1074 *Arenicola marina* irrigation behavior to oxygen transport
1075 and dynamics in sandy sediments. Journal of Marine
1076 Research 64: 915–938.
- 1077 Vedel, A. & H. U. Riisgard, 1993. Filter-feeding in the poly-
1078 chaete *Nereis diversicolor*: growth and bioenergetics.
1079 Marine Ecology Progress Series 100: 145–152.
- Vismann, B., 1990. Sulfide detoxification and tolerance in *Ne-*
reis (Hediste) diversicolor and *Nereis (Neanthes) virens*
(Annelida: Polychaeta). Marine Ecology Progress Series
59: 229–238.
- Wenzhöfer, F. & R. N. Glud, 2004. Small-scale spatial and
temporal variability in coastal benthic O₂ dynamics: effects
of fauna activity. Limnology and Oceanography 49(5):
1471–1481.
- Zhu, Q., R. C. Aller & F. Yanzhen, 2006. A new ratiometric,
planar fluorosensor for measuring high resolution, two-
dimensional pCO₂ distributions in marine sediments.
Marine Chemistry 101(1–2)(40): 40–53.

1080
1081
1082
1083
1084
1085
1086
1087
1088
1089
1090
1091
1092
1093

UNCORRECTED PROOF